Integration of H05 and H16 products through SM2RAIN algorithm for improving rainfall estimate

Associated Scientist Activity in the framework of the Satellite Application Facility on Support to Operational Hydrology and Water Management (H-SAF)

FINAL REPORT

15 December 2015

Luca Brocca[1], Luca Ciabatta[1], Christian Massari[1], Tommaso Moramarco[1], Silvia Puca[2], Davide Melfi[3], Francesco Zauli[3]

[1] Research Institute for Geo-Hydrological Protection, National Research Council, Perugia, Italy
[2] National Department of Civil Protection, Rome, Italy
[3] Italian Air Force Meteorological Service, C.N.M.C A. - Satellite Section, Pomezia (Roma), Italy

The EUMETSAT Network of Satellite Application Facilities

H SAF
Support to Operational Hydrology and Water Management

Table of Contents

1 Introduction

Owning accurate rainfall estimates is of paramount importance as rainfall plays a key-role in many fields like, to cite a few, natural hazard assessment (floods and landslides), drought management, weather forecasting, agriculture and diseases prevention (Dinku et al., 2007). State-of-the-art rainfall products obtained by satellites are often the only way for measuring rainfall in remote area of the world. The retrieval of rainfall in the state-of-the-art products is based on a "top-down" approach, i.e., rainfall is obtained through the inversion of the atmospheric signals scattered or emitted by atmospheric hydrometeors (Kucera et al., 2013). Therefore, the instantaneous rainfall rate is estimated at the overpasses of microwave sensors (radiometers and radars) and then blended between successive overpasses by using infrared measurements from geostationary satellites (Kidd and Levizzani, 2011). However, if microwave sensors do not pass when it rains, these algorithms are unable to capture the rainfall events thus underestimating the cumulated rainfall (**Figure 1**), mainly for convective precipitations events.

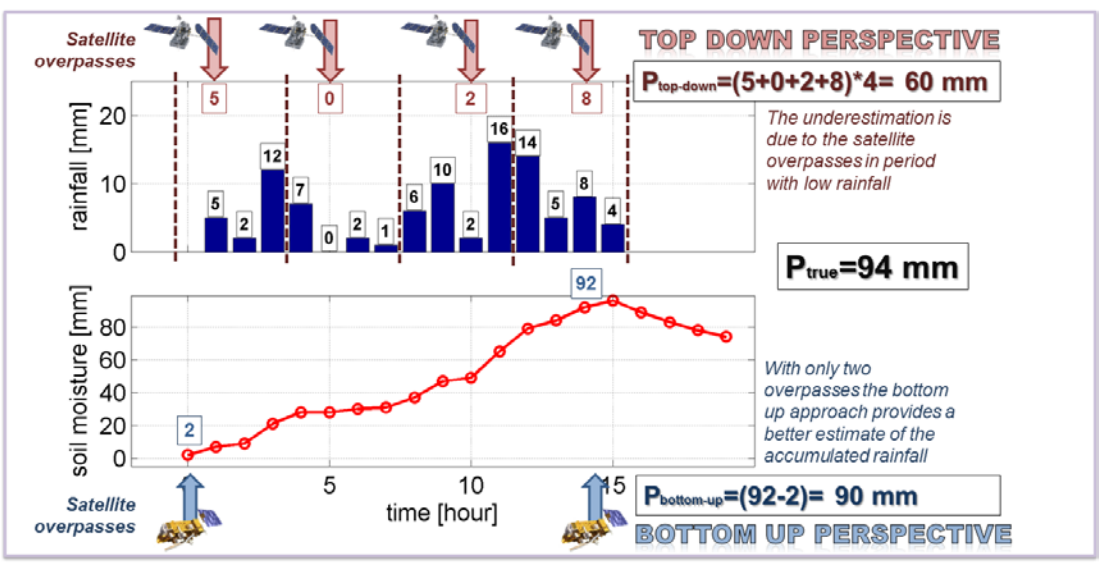

Figure 1: Bottom up vs Top down perspective for rainfall retrieval from remote sensing assuming no error in the satellite measurements and in the retrieval algorithms. Due to the satellite overpasses during low rainfall intensities, the "top down" method fails in estimating the cumulated rainfall while the "bottom up" approach well reproduce the observed value even with a lower number of overpasses.

Therefore, state-of-the-art rainfall products may fail in properly reproducing the amount of precipitation reaching the ground, which is of paramount importance for hydrological applications. Currently, one of the major issues for rainfall retrieval from space is related to the estimation of light rainfall that causes a general underestimation of rainfall accumulations (Hou et al., 2014). This issue is particularly important over land due to the uncertainty and spatial variability of surface emissivity (Tapiador et al., 2012).

With the purpose of improving the accuracy of satellite rainfall products, three approaches using satellite soil moisture data were recently developed (Crow et al., 2009; Pellarin et al., 2013; Brocca et al., 2013; Wanders et al., 2015). In the approaches of Crow et al. (2009), Pellarin et al. (2013), and Wanders et al. (2015), satellite soil moisture data are assimilated into a land surface model (simplified Antecedent Precipitation Index in Crow et al., 2009; Pellarin et al., 2013), in order to correct the 1-10 days rainfall accumulation obtained from a state-of-the-art rainfall product (i.e., 3B42-RT from TMPA - TRMM Multi-satellite Precipitation Analysis product). Therefore, these methods require a previous estimate of rainfall (first guess) that significantly affects the final results. In other words, the final rainfall estimate is strongly dependent on the first guess.

More recently, Brocca et al. (2013, 2014) proposed a novel bottom-up approach for estimating rainfall using satellite soil moisture observations, called SM2RAIN. The method is based on the inversion of the soil water balance equation. That is, it estimates the rainfall by using the change in time of the amount of water stored into to the soil, thus considering “soil as a natural raingauge”. Therefore, soil moisture data are not used to correct rainfall as in previous approaches, but directly to estimate rainfall. SM2RAIN has been applied both on a local scale with in situ observations (Brocca et al., 2013; 2015a) and on a regional (Abera et al., 2015; Brocca et al., 2015b) and a global scale (Brocca et al., 2014) with satellite soil moisture data. Specifically, SM2RAIN was successfully applied to satellite products from L- and C-band radiometers (SMOS - Soil Moisture and Ocean Salinity, AMSR-E – Advanced Microwave Scanning Radiometer Earth Observing System) and C-band (ASCAT - Advanced SCATterometer) scatterometer (Brocca et al., 2014), and the ASCAT soil moisture product provided the best performance. More recently, Ciabatta et al. (2015a) demonstrated that integrating the bottom-up and top-down (state-of-the-art products) approaches, a significant improvement in rainfall estimation could be obtained (see **Figure 2**). Moreover, Massari et al. (2014), in a small catchment in southern France, found that the

correction of rainfall through SM2RAIN, applied to in situ soil moisture observations, provides improvement in flood modelling when compared to the use of rain gauge observations only. Similar results were obtained by Ciabatta et al. (2015b) in 4 different catchments throughout Italy but applying the method to satellite observations.

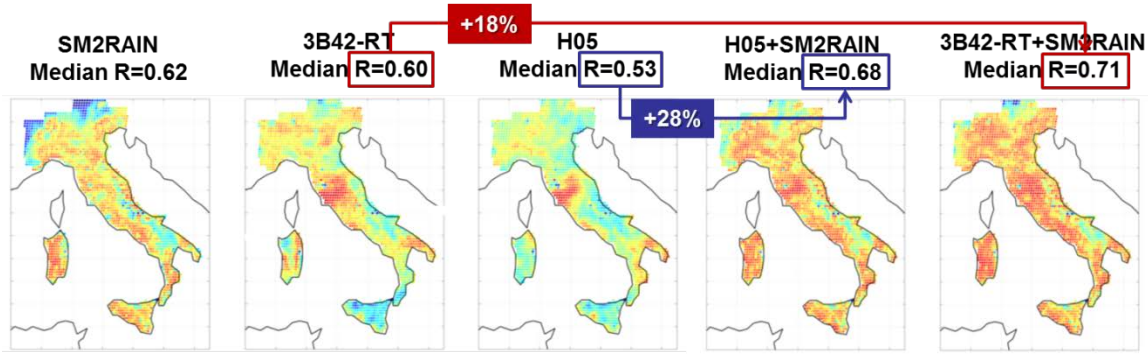

Figure 2: Correlation maps between satellite-derived and observed 5-day rainfall over the validation period 2012-2013 for (from left to right): 1) SM2RAIN applied to ASCAT soil moisture data, 2) 3B42-RT (TMPA product), 3) H05 (H-SAF product), 4) integrated product SM2RAIN-ASCAT+H05, and 5) integrated product SM2RAIN-ASCAT+3B42-RT. The improvements in median correlation values from parent (H05 and 3B42-RT) and integrated products are also highlighted (figure adapted from Ciabatta et al., 2015a).

The capability of SM2RAIN approach to estimate rainfall by using the variation in soil moisture between two different satellite passages represents an important advantage, with respect to classical retrieval methods, in terms of estimating the cumulated rainfall value over a period, e.g., 1-5 days (see **Figure 1**) (Ciabatta et al., 2015a). As mentioned before, in the top-down satellite-based algorithms (e.g. PR-OBS-5 and 3B42-RT), the instantaneous rainfall rate is estimated with possible issues in capturing the total amount of rainfall fallen over a period due to the very high temporal variability of rainfall. When using satellite soil moisture data, the amount of rainfall fallen into the soil is recorded and, hence, by computing the difference in the water storage, the cumulated rainfall is estimated (note that SM2RAIN has also an additional component for taking into account the vertical percolation of the soil layer). This allows to keep track of the total rainfall fallen between satellite passages (without losing water), with an expected higher degree of accuracy.

However, SM2RAIN method may fail in reproducing rainfall when the soil is close to saturation (Brocca et al., 2013) and if the temporal resolution of the data is too

coarse (e.g. >2-3 days). Indeed, for obtaining rainfall products at high temporal resolution (daily, sub-daily) through the SM2RAIN algorithm, soil moisture retrievals from multiple sensors are needed to achieve 4-8 overpasses per day. Moreover, the method is strongly dependent on the accuracy of the original satellite soil moisture dataset used as input. Therefore, high errors are expected in mountain, urbanized and highly vegetated areas and during frozen/snow soil conditions (Brocca et al., 2014, Ciabatta et al., 2015a).

Based on the discussion reported above, it seems obvious the huge potential that can be obtained by merging top-down and bottom-up approaches. Indeed, the two approaches have complementary features that would allow maximizing the accuracy in rainfall estimation through their integration. The integrated product is expected: 1) to provide higher accuracy in the spatial and temporal estimation of cumulated rainfall over a period of 1-5 days, and 2) to be slightly affected by complex conditions at the surface (mountains, high vegetation, urban areas, frozen conditions, soil saturation).

Therefore, the main purpose of the proposed Associated Scientist Activity (ASA) is the development of a new cumulated rainfall product (over 24 hours) that integrates satellite rainfall and soil moisture (through SM2RAIN) datasets by considering two operational products delivered within the H-SAF project: PR-OBS-5 (i.e., H05 – ATDD-05, 2010) and SM-OBS-3 (i.e., H16 - ATBD-16, 2013). Specifically, the ASA is dedicated to the application of SM2RAIN algorithm to H16 for providing the SM2RAIN-derived product, named P_H16. Then, the latter is integrated to H05 through an optimized nudging scheme that takes into account the error structure of the two products. The new integrated product, i.e. H05+P_H16, is validated with ground rainfall observations across Europe (E-OBS, Haylock et al., 2008). Finally, the operational implementation, the specifications (e.g. spatial-temporal resolution) and the requirements of the integrated product are briefly discussed.

2 Study area and data sets

Two rainfall datasets (one from satellite data, H05, and one from raingauge data, EOBS, Haylock et al., 2008) and one satellite soil moisture dataset, H16, characterized by different temporal and spatial resolutions, are considered in the period 10 May 2013 – 31 December 2014. The study region is the whole European country with also a small part in northern Africa (see **Figure 3**).

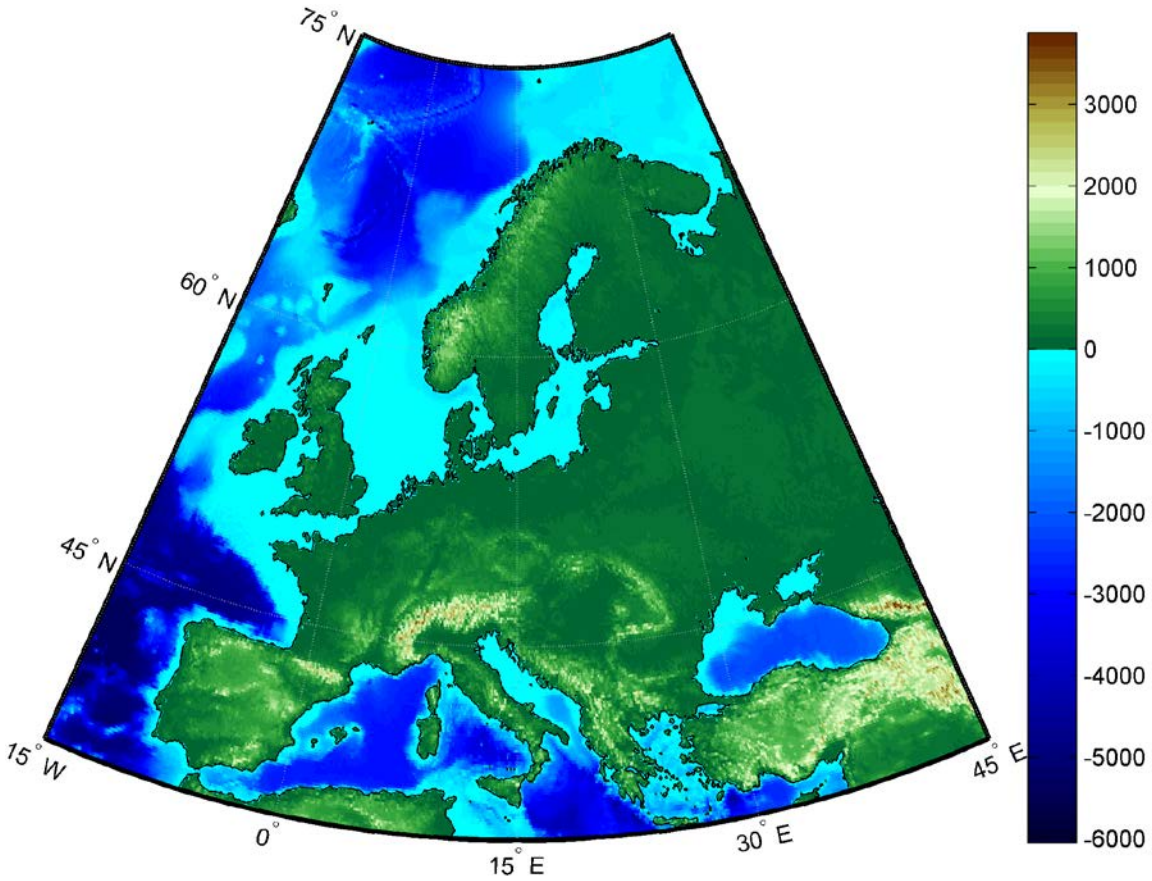

Figure 3: Elevation map of the study area selected for this study.

In order to match the different temporal and spatial resolutions of the different products, each of them is remapped (through the nearest neighbour algorithm) over a regular grid with spacing of 12.5 km (57695 grid points in total for the selected study area, **Figure 4**). For this study, the selected spacing is based on the coarser grid of the two selected datasets (H05 and H16). Concerning the remapping methodology, different techniques have been used at the beginning of this study (Nearest Neighbour, Inverse Distance Weighted, and Kriging) and we

found that the Nearest Neighbour method provides satisfactory results in a very short computational time. The cumulated daily rainfall between 00:00 UTC and 24:00 UTC is computed for each rainfall product, while the soil moisture data are interpolated in time at 00:00 UTC in order to match the temporal resolution of the rainfall datasets. In **Table 1** a summary of the datasets spatial and temporal resolutions considered in this study is reported.

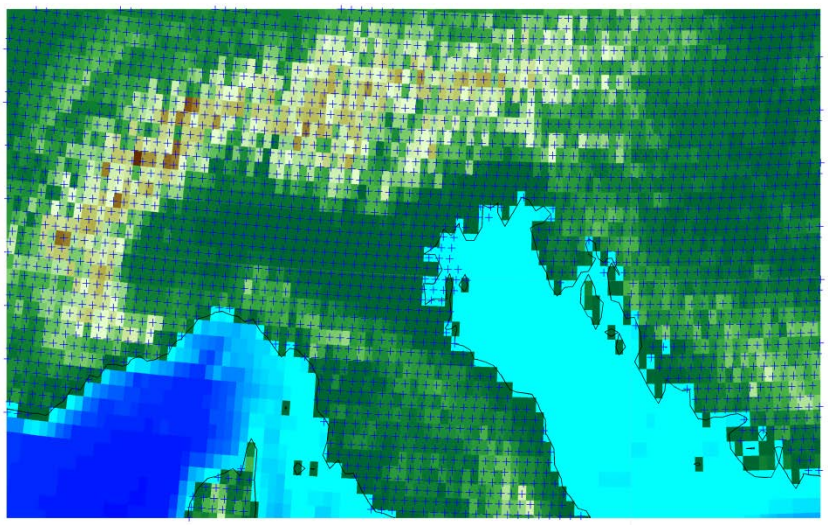

Figure 4: Example of the regular grid (with spacing ~12.5 km) selected for the remapping of the different products.

Table 1: Main characteristics of the satellite datasets used in this study (MW: Microwave, IR: infrared, ASCAT: Advanced SCATterometer).

Dataset	*Product*	*Spatial resolution*	*Temporal resolution*
E-OBS v12.0	Gauge-based rainfall	0.22° rotated grid	Daily
H05	MW+IR merged product	~5 km	Daily
H16	ASCAT soil moisture	~12.5 km	~Daily

2.1 Ground-based rainfall dataset

The European daily high-resolution gridded data set of precipitation, surface maximum, mean, and minimum temperatures, E-OBS (Haylock et al., 2008), was developed as part of the EU-FP6 ENSEMBLES project, with the aim to use it for validation of Regional Climate Models (RCMs) and for climate change studies. The data were interpolated from the largest available pan-European data set of about 2300 stations involved in the ECA&D project (Klok and Klein Tank, 2008); E-OBS version 12.0 is examined in this study. The exact number of stations varies over time and is larger for precipitation than temperature (Haylock et al., 2008). The station spatial coverage is uneven (see Figure 1 in Haylock et al., 2008); areas with high density of stations include mainly the United Kingdom and parts of Western Europe, whereas low density is typical of the Iberian Peninsula, south-eastern and northern Europe. In the recent versions (10, 11, 12), the number of stations used has increased (see http://www.ecad.eu/download/ensembles/download.php). The E-OBS data set was designed to provide best estimates of grid box averages rather than point values to enable direct comparison with RCMs. The daily data were interpolated using a three-step methodology. First, monthly means were interpolated to a high-resolution 0.1° × 0.1° rotated pole grid using three-dimensional thin-plate splines to define the underlying spatial trend of the data. The next step was kriging the anomalies with regard to the monthly mean; for all days a single variogram was used. Elevation dependencies were incorporated by using external drift kriging. The final result was created by applying the interpolated anomaly to the interpolated monthly mean. The 0.1° points were used to compute area-average values at the final E-OBS grid resolutions (of about 50 and 25 km, Haylock et al., 2008). The data were gridded onto four different grids. The grid examined in this study is the 0.22° rotated pole grid. The E-OBS data set was originally produced to cover the period 1950-2006 and later updated to June 2015 (version 12). We examine the data over 2013-2014, that is, the period corresponding to the satellite soil moisture dataset.

2.2 Satellite rainfall product

The H05 product is provided by the European Organisation for the Exploitation of Meteorological Satellites (EUMESAT) within the “Satellite Application Facility on Support to Operational Hydrology and Water Management” (H-SAF, http://hsaf.meteoam.it/) project. The product is based on frequent precipitation

measurements as retrieved by blending Low Earth Orbit (LEO) microwave (MW) derived precipitation rate measurements and Geostationary Earth Orbit (GEO) infrared (IR) imagery. This product provides daily rainfall data with a spatial resolution of ~5 km over the H-SAF area (25°N–75°N latitude, 25°W–45°E longitude) covering the whole European continent, Iceland and northern Africa. The cumulated daily rainfall between 00:00 UTC and 24:00 UTC is considered here consistently with E-OBS dataset.

2.3 Satellite soil moisture data

The surface soil moisture data are obtained by backscattering retrievals from the ASCAT sensor (C-band scatterometer operating at 5.4 GHz) onboard the Metop-A and Metop-B satellites. In this study, the WAter Retrieval Package (WARP) at version 5.51 is used for estimating soil moisture from backscatter measurements (H16 product). Currently, the H16 product is archived in the EUMETcast dissemination system and can be downloaded through the "EUMETSAT Data Centre Online Ordering" application. H16 data are stored in orbit files and can be downloaded in different format (NetCDF, HDF5, EPS). For this analysis, the orbit data passing over Europe from Metop-A and Metop-B satellites have been downloaded in NetCDF format from 10th May, 2013 to 31st January, 2015. The data are processed for passing from orbit files to a regular grid with spacing ~12.5 km (see **Figure 4**), that is the same grid used for the H25 (METOP ASCAT Soil Moisture Time Series) product. The interpolation is simply carried out with the nearest neighbouring method. Finally, the gridded H16 data are stored in a Matlab file ".mat" and made available in the FTP of H-SAF project (e.g., for the delivering of the "Product Validation Report" of H16 available at http://rs.geo.tuwien.ac.at/validation/H16/report.html). We note here that the official H16 product in the H-SAF project is the one obtained by using Metop-B satellite data only. However, we used here both Metop-A and Metop-B satellites for increasing the temporal resolution of the data that has a strong beneficial effect on SM2RAIN algorithm.

By considering both Metop-A and Metop-B satellites, the product has on average more than on passes per day even though the time difference between Metop-A and Metop-B is usually less than 1 hour. Due to the variable temporal resolution of the surface soil moisture product, all the soil moisture data have been interpolated in time at 00:00 UTC each day. This step allows to compare all the

datasets considered in this study in a consistent manner, i.e. the daily cumulated rainfall from 00:00 UTC to 24:00 UTC is obtained for each product.

2.4 Final selection of the study region

The consistency between rainfall and soil moisture datasets is firstly analysed to perform the intercomparison in the space domain where all products have good spatial coverage. Indeed, while the soil moisture dataset (H16) is found to be complete (no missing data), H05 and E-OBS have a significant number of missing data in some specific regions (blue areas in **Figure 5**). Therefore, the following analyses are carried only considering the pixels with more than 400 valid data for both H05 and E-OBS products, thus excluding 13530 points. The final number of grid cells is equal to 44165.

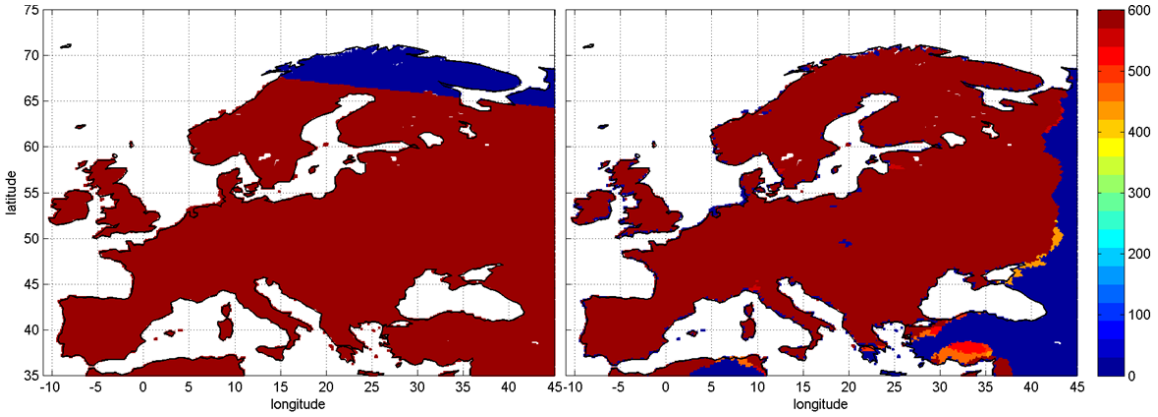

Figure 5: Sample size of H05 (left) and E-OBS (right) rainfall datasets over the period from 10-May-2013 to 31-December-2014.

3 Methods

To accomplish the purpose of the ASA two different methods are implemented: 1) the SM2RAIN algorithm, and 2) the nudging scheme.

3.1 SM2RAIN

The SM2RAIN method is based on the inversion of the following water balance equation (Brocca et al., 2015a):

$$\frac{Znds(t)}{dt} = p(t) - r(t) - e(t) - g(t)$$

where *Z* [L] is the soil depth, *n*[-] is the soil porosity, *s(t)* [-] is the relative saturation of the soil or relative soil moisture, *t* [T] is the time and *p(t), r(t), e(t)* and *g(t)* [L/T] are the precipitation, surface runoff, evapotranspiration and drainage rates, respectively. By assuming that during rainfall the surface runoff and the evapotranspiration rates are negligible, and by considering *Z*=Zn*, the rainfall rate is obtained as:

$$p(t) \cong \frac{Z^* ds(t)}{dt} + as(t)^b$$

Where the drainage rate is expressed as a non-linear function of the soil saturation [*g(t)=as(t)^b*]. The *Z**, *a* and *b* parameters are considered varying in space and are estimated through calibration against benchmark rainfall observations. The reader is referred to Brocca et al. (2015a) for a detailed description of SM2RAIN algorithm.

3.2 Exponential filter

Satellite soil moisture observations are sensitive to a very thin soil layer (<2-5 cm) that might be not sufficient for detecting the temporal changes of soil moisture due to rainfall. To address this issue, the semi-empirical approach, known as exponential filter, proposed by Wagner et al. (1999) is adopted to obtain a root-zone soil moisture product (SWI, Soil Water Index) that depends on a single parameter, *T* (characteristic time length) representing the time scale of soil moisture variation. The *T*-value can be either obtained from calibration (e.g. maximizing the correlation with in situ observations or modelled data) or fixed a

priori by considering the results already published in the scientific literature (Wagner et al., 1999; Albergel et al., 2009; Brocca et al., 2011). In this study, the *T*-value is calibrated together with the three parameter of SM2RAIN algorithm in order to maximize the agreement with benchmark rainfall observations. The reader is referred to Wagner et al. (1999) and Albergel et al. (2009) for a detailed description of the exponential filter approach.

3.3 Nudging scheme

The integration of the rainfall datasets, *P_H16* and *H05*, is implemented by using the following nudging scheme:

$$H05 + P\_H16(t) = P\_H16(t) + K[H05(t) - P\_H16(t)]$$

where *H05+P_H16(t)* is the integrated rainfall product and *K* is the gain parameter, ranging between 0 and 1; for *K*=0 only the estimated rainfall through SM2RAIN, *P_H16* is used, for *K*=1 only *H05*. *K* is calibrated by maximizing R between observed and integrated rainfall considering 1 day of cumulated rainfall and following the method given by Kim et al. (2015).

3.4 Performance metrics

In order to evaluate the performance of the rainfall products, the correlation coefficient (R), the BIAS and the root mean square error (RMSE) values over 1 and 5 days of cumulated rainfall are computed separately for each grid point to assess the spatial variability of the products performance in time. Moreover, the spatial R values for each day and for 1 day of cumulated rainfall are computed, to assess the products capability to reproduce the observed rainfall spatial pattern. Also, three categorical metrics are computed, considering the same durations: the Probability Of Detection (POD), the False Alarm Ratio (FAR) and the Threat Score (TS). The first refers to the fraction of all correctly predicted events, the second to the fraction of predicted events that are actually non-events and the third gives an integrated information of the overall performance. Following Brocca et al. (2014), the categorical scores are computed for each point and for different rainfall thresholds computed as percentiles of the observed rainfall timeseries. Therefore, categorical scores are evaluated as a function of rainfall intensity for understanding products performance in capturing low to high rainfall events.

4 Results

In the sequel, three rainfall datasets are evaluated (**Table 1**). Specifically, the H05 and the H16-derived (P_H16) products are considered along with the product obtained from the integration of satellite rainfall and soil moisture data (P_H16+H05). The analysis is carried out during the period from 10 May 2013 to 31 December 2014 without considering a calibration and a validation period in order to maximize the sample size used for analysing the results. The main constraint is due to the availability of Metop-B observations (from May 2013). In the near future, the developed products will be evaluated by using the more recent data.

4.1 Rainfall estimation from H16 soil moisture product through SM2RAIN

The SM2RAIN parameter values, along with the *T*-parameter of the exponential filter, are obtained through a spatially distributed pixel-by-pixel calibration. Specifically, E-OBS data are used as benchmark and the minimization of the RMSE for cumulated rainfall over 5 days is selected as objective function. **Figure 6** shows the spatial distribution of the obtained parameter values. The *Z** parameter shows the highest values in the areas characterized by the highest rainfall regime in good accordance with Brocca et al. (2014) and Ciabatta et al. (2015a) who obtained *Z** increasing with the rainfall amount in the pixel. The *a* parameter shows sometimes high values along the coastline and this "coast-effect" could be traced to the satellite soil moisture retrievals issues at the water-land interface. The *b* parameter shows quite high values (>40) with a spatial pattern somehow complementary to *a* values. It is likely due to the role of *a* and *b* parameters in determining the intensity of the drainage rate (see section 3.1); indeed drainage increase with increasing *a* and *b* values. Finally, *T*-values agree with the spatial pattern of *Z**. Indeed, for generating higher rainfall rates, a deeper soil layer should be considered and, hence, higher valued for both *Z** and/or *T*. The SM2RAIN parameters show mean values of 127.6 mm, 17.9 mm/day, 56.3 and 11.0 days for *Z*, a, b*, and *T*, respectively. The mean values of *Z** is higher than those obtained in Brocca et al. (2014) and Ciabatta et al. (2015a), lower than 65 mm, and it is clearly due to the application of the exponential filter that allows to obtain a soil moisture estimate for a deeper soil layer. Conversely, *a* and *b* show values lower than Ciabatta et al. (2015a) as after the application of the exponential filter the noise of satellite soil moisture

data are reduced, similarly to the effect of spatial averaging as carried out in Brocca et al. (2014). Indeed, it is obtained that reducing the noise in the soil moisture data, the *a* and *b* parameters show low values.

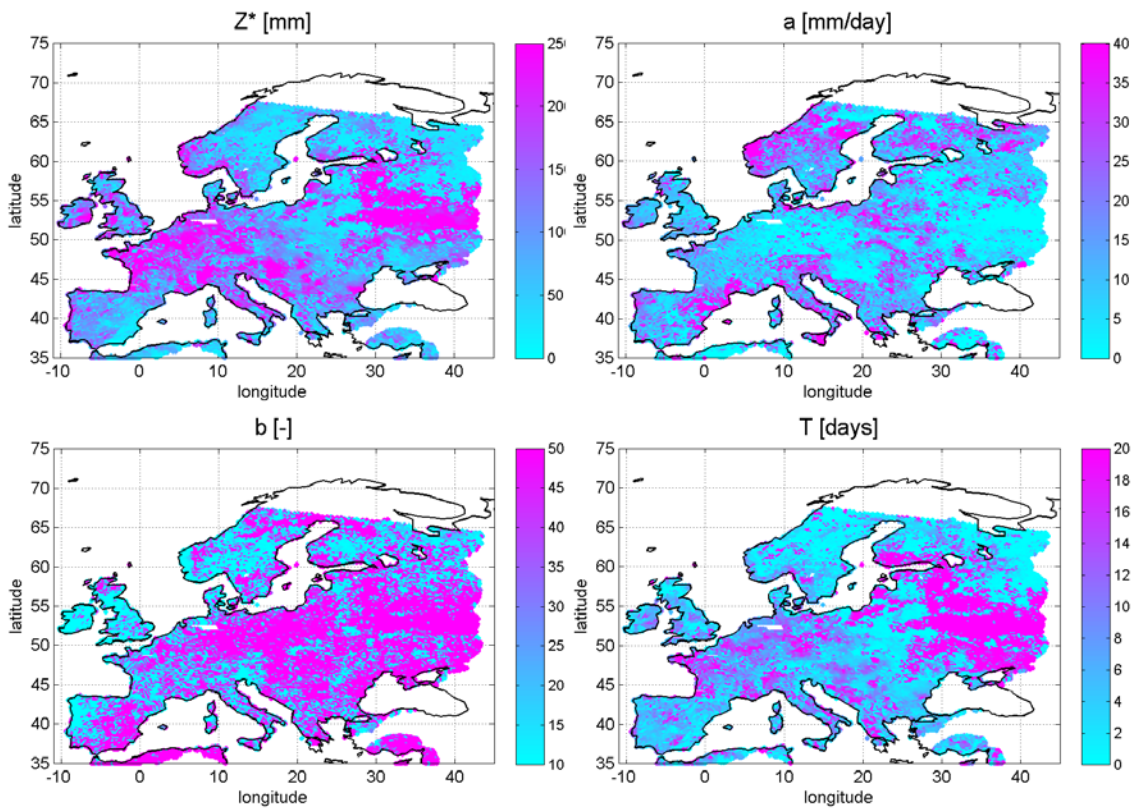

Figure 6: Spatial distribution of SM2RAIN parameter values obtained through the calibration against E-OBS data in the period May 2013-Dec 2014.

In summary, a good agreement between the obtained parameter values and previous studies is found and it allows us to conclude that the obtained parameterization can be robust and consistent also for the actual implementation of the P_H16 product integrated with H05. Further studies should be addressed to evaluate the relationship between the SM2RAIN parameters, soil texture, vegetation and grid resolution using high resolution soil and land use map.

As a first comparison, the cumulated rainfall map over the whole analysed period is shown in **Figure 7** for E-OBS and P_H16 products. The agreement between the two maps is quite good with the clear detection from the P_H16 product of the regions with higher (e.g., in western Scandinavia, north-western UK and Spain, Alps and Pyrenees) rainfall accumulations. Some differences can be

detected over the western Alps, and in Eastern Europe in which P_H16 product seems to underestimate the cumulated rainfall.

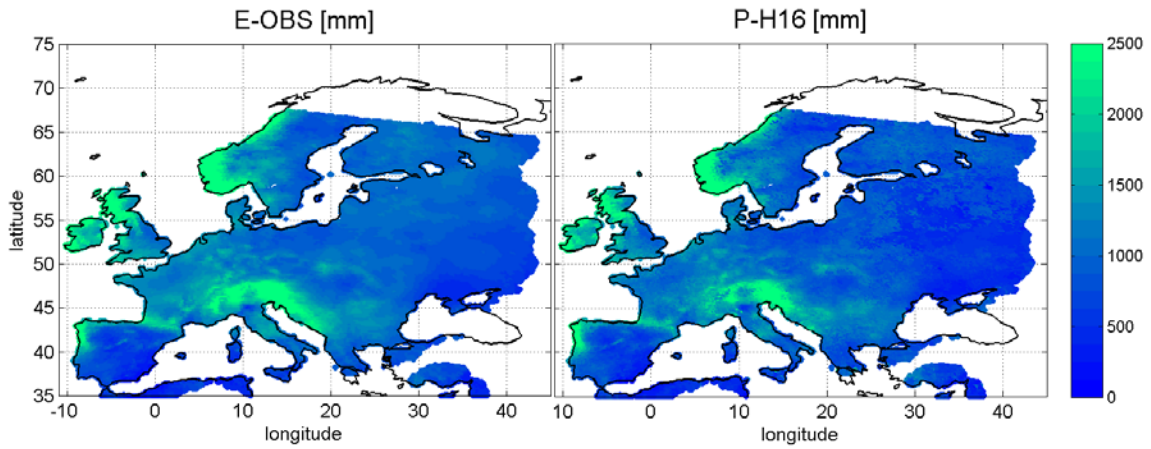

Figure 7: Cumulated rainfall over the period May 2013-Dec 2014 for E-OBS (left) and P_H16 (right) rainfall products.

4.2 Performance of H05 and P_H16 products

Before to develop and analyse the integrated product, the performance of the parent products alone is investigated. **Table 2** shows the main statistics of the performance scores (R, RMSE, BIAS, and TS) for each analysed product and for 1-day and 5-day cumulated rainfall. Overall, the performance of both H05 and P_H16 products is satisfactory and it demonstrates the good performance of the products in reproducing the daily cumulated rainfall throughout Europe at the spatial scale of ~20 km. In details, H05 (P_H16) product has slightly better performance for 1-day and 5-day cumulated rainfall in terms of temporal correlation but with differences in median R values less than 0.04. In terms of RMSE, P_H16 provides significantly better performance than H05 for both durations. This result is expected as P_H16 is calibrated to minimize RMSE against E-OBS rainfall data whereas it is not the case for the H05 product. Therefore, the obtained results for H05 should be considered as an independent validation. H05 provides also better performance in terms of TS (computed for a rainfall threshold of 0.0 mm) and of BIAS, while it is the opposite for the absolute BIAS (**Table 2**).

Table 2: Summary statistics of the performance scores of the different satellite rainfall products in the comparison with E-OBS data (R: correlation coefficient, RMSE: root mean square error, TS: Threat Score for a rainfall threshold of 0.0 mm, 10°,50°,90°: 10th, 50th, 90th percentiles).

		1-day rainfall			*5-day rainfall*			*BIAS (%)*	*|BIAS| (%)*
		R	RMSE (mm)	TS	R	RMSE (mm)	TS		
H05	90°	0.61	6.49	0.59	0.74	15.68	0.88	53.1	56.3
	50°	0.50	4.64	0.51	0.63	10.75	0.78	10.0	21.9
	10°	0.35	3.57	0.40	0.48	7.96	0.63	-29.5	4.3
P_H16	90°	0.63	5.19	0.53	0.79	12.02	0.84	1.1	34.4
	50°	0.46	3.41	0.40	0.62	8.17	0.74	-11.8	12.5
	10°	0.24	2.59	0.29	0.41	5.89	0.56	-34.3	2.7
H05 + P_H16	90°	0.71	4.79	0.59	0.84	11.05	0.87	28.2	31.9
	50°	0.60	3.23	0.47	0.74	7.32	0.77	-0.5	12.2
	10°	0.42	2.58	0.33	0.58	5.62	0.57	-21.1	2.2

The spatial distribution of the R-values for the whole study area is shown in **Figure 8** for both products and durations. As it can be seen, the performance of P_H16 is strongly related to the surface conditions. Lower performance is obtained over the mountains (Alps and Pyrenees), at high latitudes due to frozen soils and the presence of snow, and also over bare soils characterized by thin soil layer above the bedrock (south-eastern Spain). In other regions, P_H16 performance is better than H05 (the median values of the two products are similar), and particularly in western Spain and France, southern UK, Benelux and Germany, and large part of Italy. Therefore, the integration of the two products is expected to provide large improvements.

Finally, the categorical scores (FAR, POD and TS) are computed for the two products by considering different rainfall thresholds computed as percentiles of observed rainfall in each pixel. Therefore, results shown in **Figure 9** and **Figure 10** highlight the capability of the two products to correctly detect observed rainfall events characterized by different intensities. Overall, H05 is performing better for low intensity rainfall events, but for higher intensities (>30°) P_H16 seems to better reproduce observed data. This behaviour is consistent for all the three categorical scores and, again, demonstrates the high complementarity of the two products.

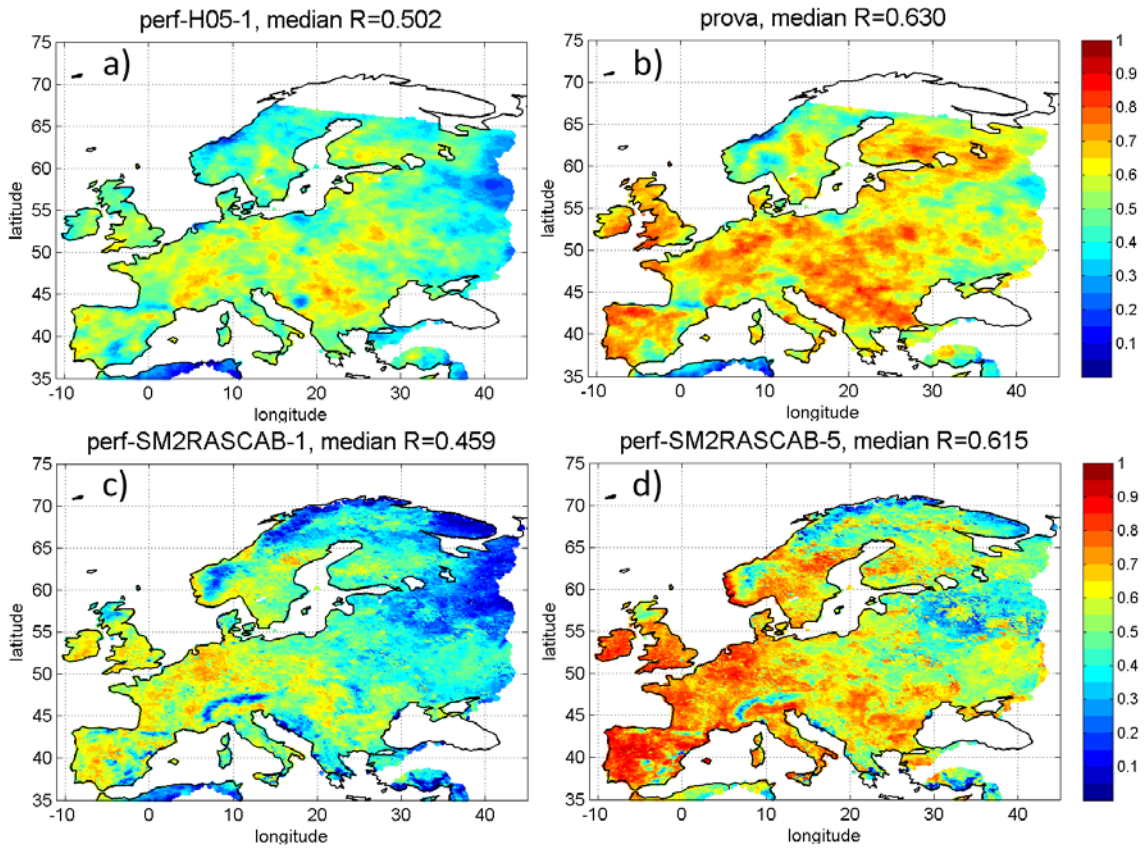

Figure 8: Correlation maps for the comparison of the H05 (a,b) and P_H16 (c,d) satellite products against E-OBS rainfall data over the period May 2013-Dec 2014 and by considering 1-day (a,c) and 5-day (b,d) cumulated rainfall.

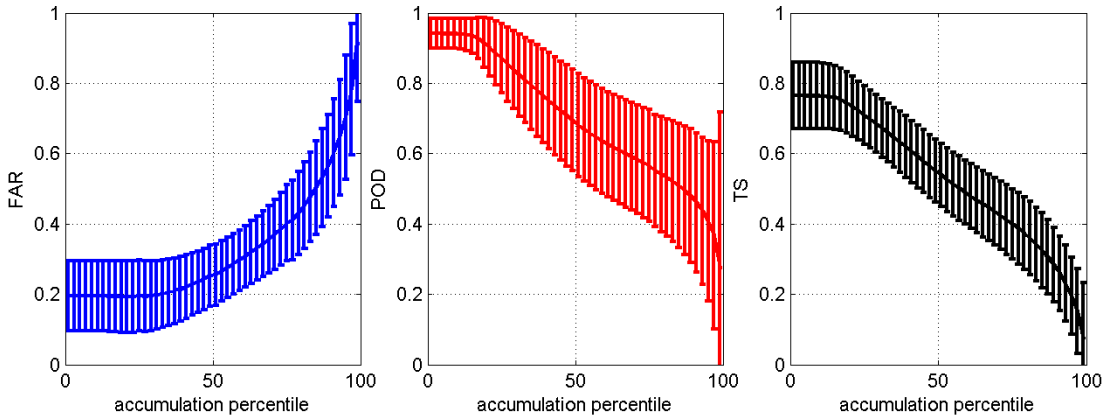

Figure 9: Summary performance of H05 product in terms of categorical scores - from left to right: FAR (False Alarm Ration), POD (Probability Of Detection) and TS (Threat Score) - as a function of different accumulation percentiles for 5-day cumulated rainfall.

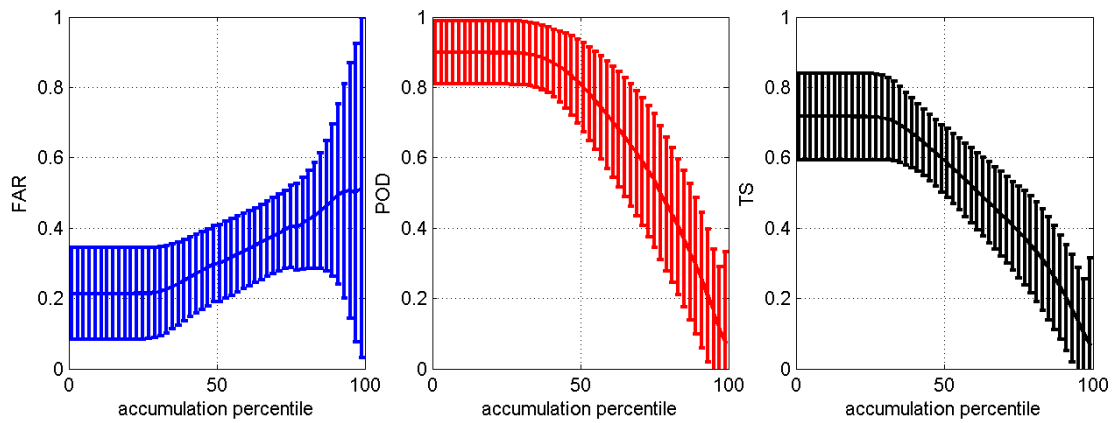

Figure 10: As in **Figure 9** but for P_H16 product.

4.3 Performance of the integrated product: H05+P_H16

As mentioned in the Methods section, the H05 and P_H16 products are merged in order to maximize the 1-day R-value pixel by pixel. In this case, the calibration is performed for 1-day rainfall, instead of 5 days, as the integrated product is found quite accurate also at fine temporal scale. **Figure 11** plots the spatial variability of *K* parameter for the integration of the two products.

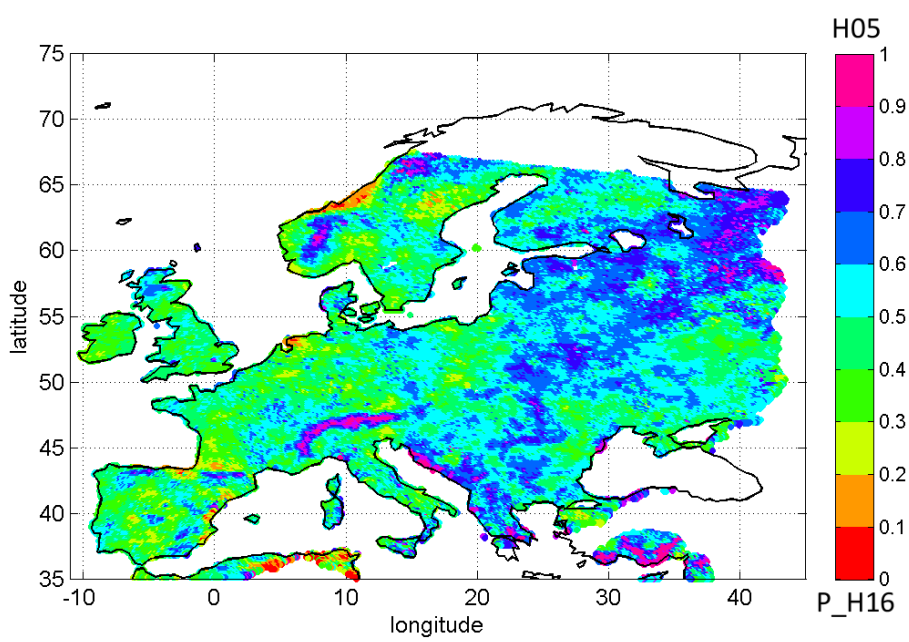

Figure 11: Map of the *K* values obtained from the integration of H05 and P_H16 (*K*=0 means only P_H16, *K*=1 only H05).

The spatial pattern of *K* is clearly related to the performance of the parent products as shown in **Figure 8**. Very high values of *K* are found in those areas where H05 significantly outperforms P_H16 (Alps, Pyrenees, Eastern Europe and southern Norway), vice versa in the remaining part of Europe *K* has values lower than 0.5 indicating a higher weight to P_H16 product.

By analysing the summary statistics of the performance scores shown in **Table 2**, it is evident the improvement related to the integration of the two products. All scores made evidence of this result with an increase in the R and TS values, and a reduction of RMSE and BIAS (also the absolute BIAS). The median values of R and RMSE are very satisfactory (R=0.6 and RMSE=7.3 mm), with improved performance with respect to the results shown by Stampoulis et al. (2012) in an evaluation of TMPA and CMORPH products over Europe.

Figure 12 shows, in the two top panels, the correlation maps for the integrated product with respect to E-OBS data for 1-day and 5-day cumulated rainfall. The results are found particularly good for nearly the whole study area. For instance, 80% of pixels show R-values larger than 0.50 and 0.65 for 1-day and 5-day cumulated rainfall, respectively. The correlations obtained for the whole Europe are even slightly better than the results shown in Italy by Ciabatta et al. (2015a). Interestingly, the two bottom panels in **Figure 12** show the ratio between the R-value of the integrated product with respect to the average performance of the parent products. The median improvement is found to be equal to 22% and 14% for 1-day and 5-day cumulated rainfall, respectively. Higher values are obtained in Eastern Europe, over mountains and near to the coasts. Some degradation is observed in the northern Africa region here analysed, however the accuracy of E-OBS in this area is expected to be quite poor thus being the results not robust. The analysis of the categorical scores (**Figure 13**) basically confirms the expectation seen in **Figure 9** and **Figure 10**, i.e., the integrated product provides an improvement of the scores for both low and high intensity rainfall events. The highest improvements seem to be obtained for the detection of larger events, which are also the most important events if satellite observations are used for the hydrological analysis of extreme conditions (e.g., floods and landslides).

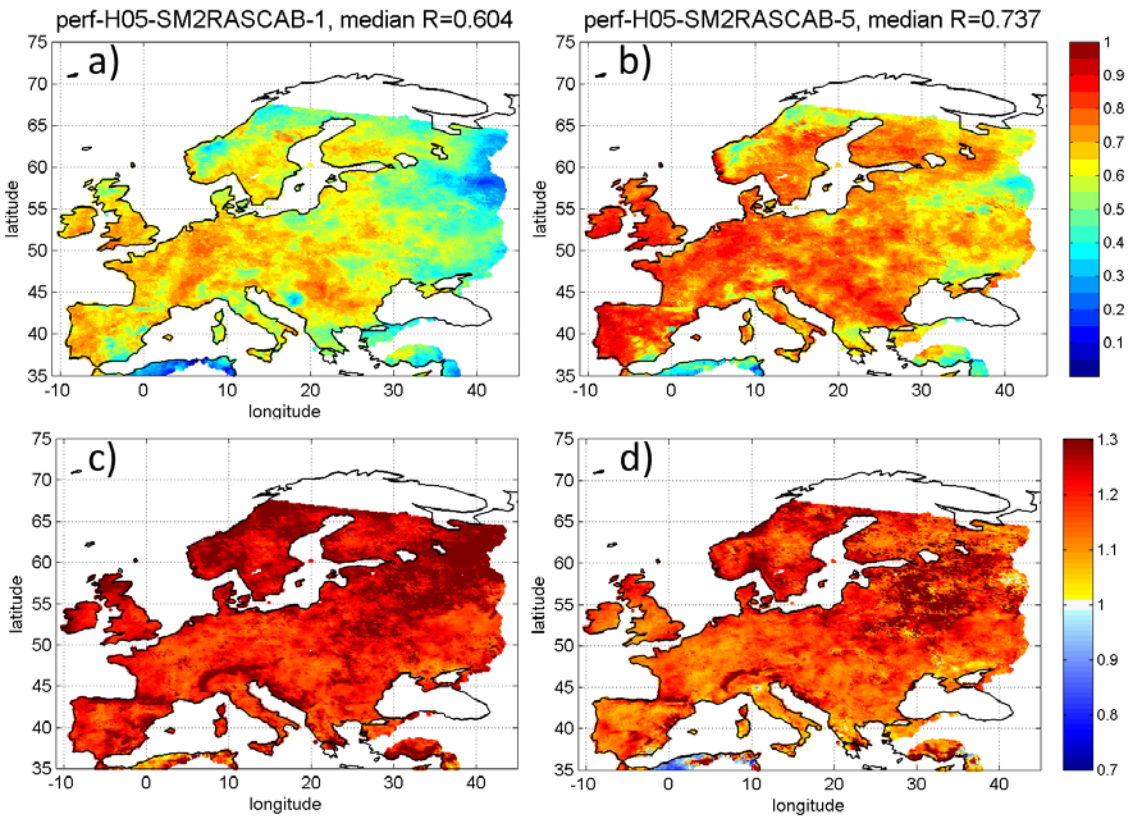

Figure 12: Correlation maps for the comparison of the H05+P_H16 (a,b) satellite product against E-OBS rainfall data over the period May 2013-Dec 2014 and by considering 1-day (a) and 5-day (b) cumulated rainfall. In the bottom panels, the ratio between the R-values obtained for the integrated product with respect to the average performance of the parent products (H05 and P_H16) is shown for 1-day (c) and 5-day (d) cumulated rainfall.

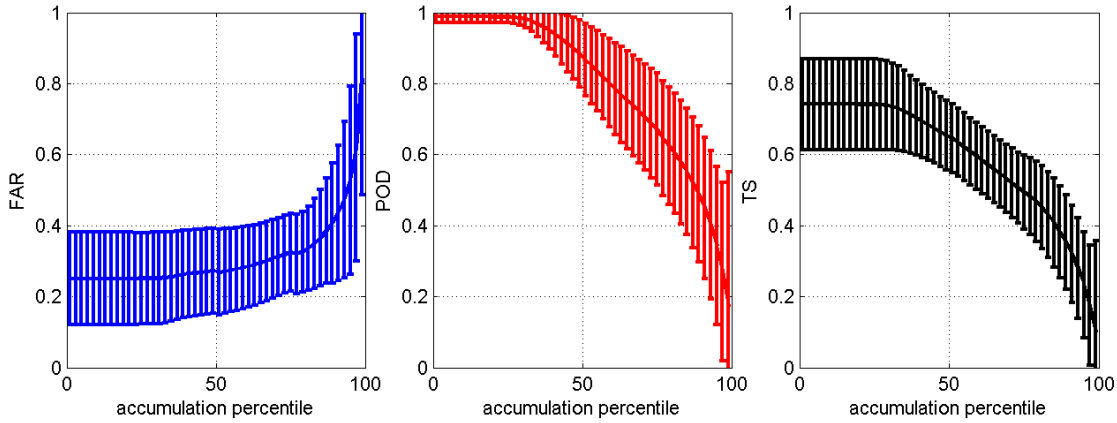

Figure 13: As in **Figure 9** but for H05+P_H16 product.

As an example, **Figure 14** shows the rainfall timeseries, for 1-day and 5-day cumulated rainfall, for some locations randomly selected in different European countries. Specifically, for making the analysis more robust, the comparison is performed by using the rainfall averaged over the nine pixels centred in the investigated location (indicated in the title). Indeed, E-OBS dataset is more representative of a grid cell of 25×25 km, and hence the comparison for a larger area is more robust. Indeed, the performances are even better than those shown in previous analyses, with most of the locations showing R-values higher than 0.7 and 0.8 for 1-day and 5-day cumulated rainfall. Quite surprisingly, good performances are also obtained for the pixels in Norway and Austria that are the areas in which the integrated product should perform worse.

Finally, **Figure 15** shows the temporal evolution of the spatial correlation between observed and satellite-deriver rainfall for each day in the investigated period May 2013-December 2014. The median spatial correlation is equal to 0.5, for daily rainfall data, with lower values occurring in December, likely due to frozen conditions in most of the study area that significantly affect the performance of P_H16 product, and hence of the integrated one. For addressing this issue, the use of temporal varying *K*-values in the nudging scheme might be considered.

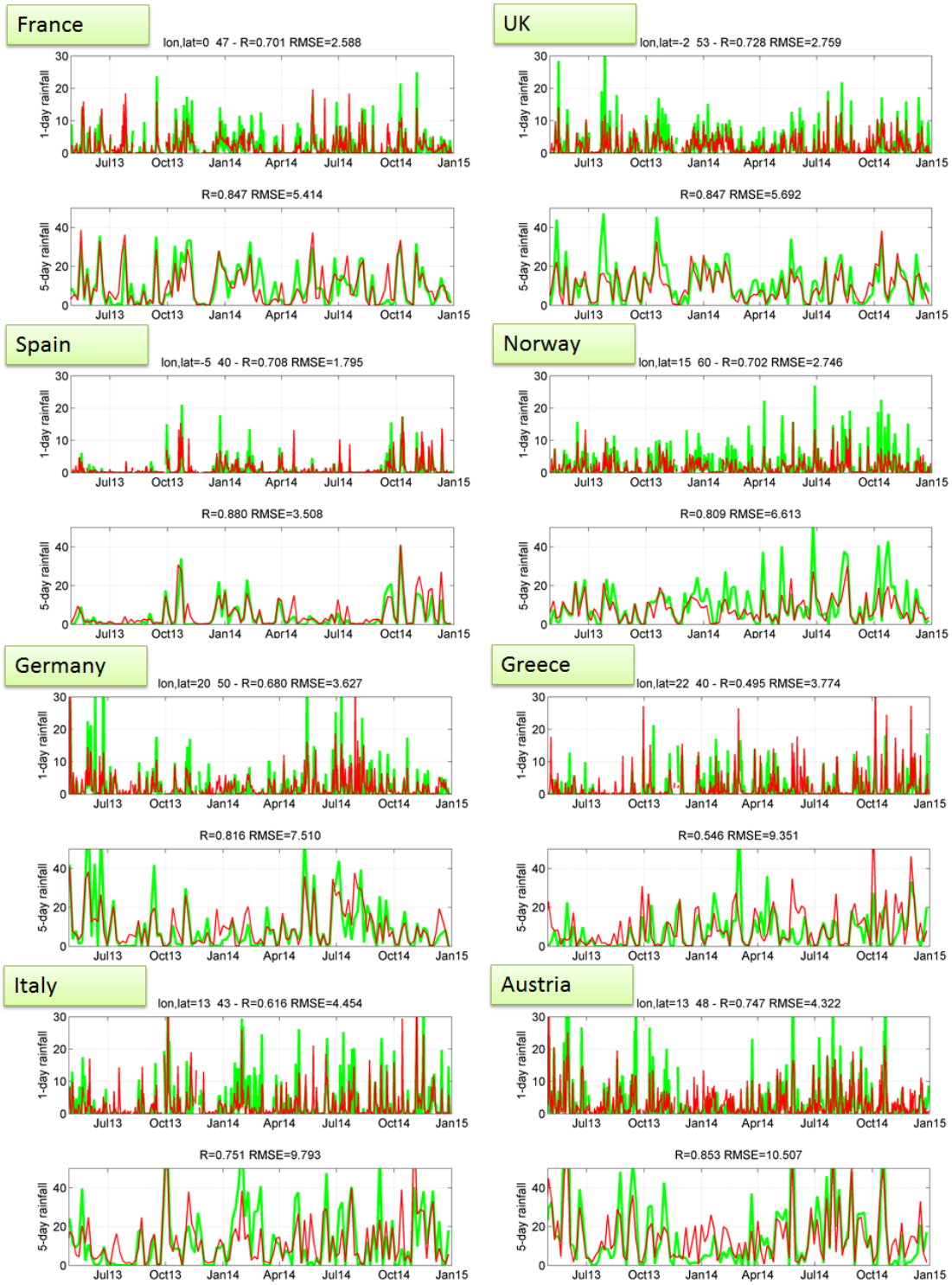

Figure 14: Comparison between observed and satellite-derived, H05+P_H16 product, rainfall timeseries for several locations across Europe for 1 and 5 days of cumulated rainfall.

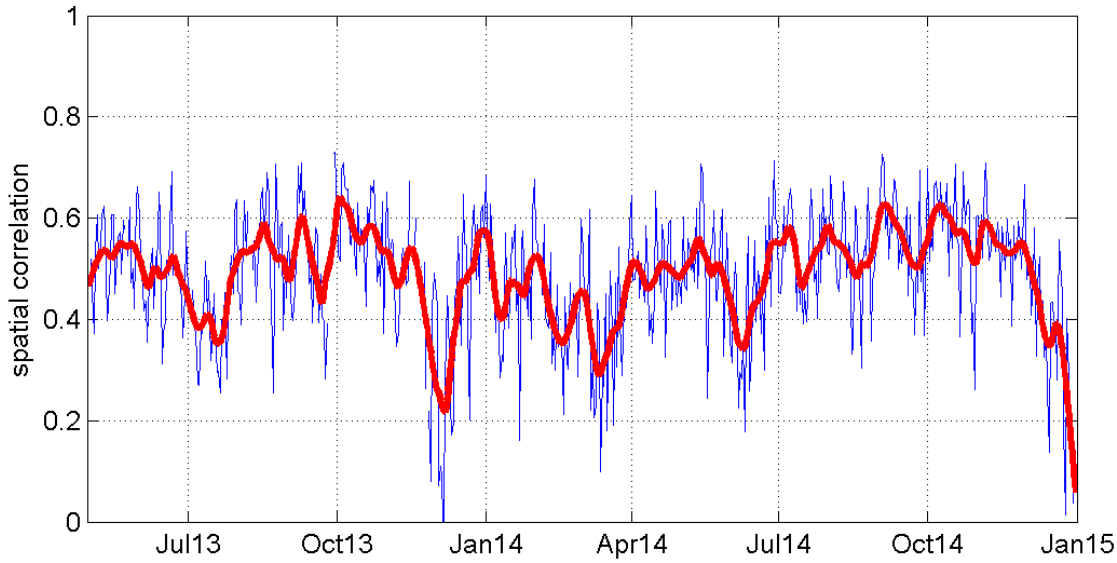

Figure 15: Temporal evolution of the spatial correlation coefficient between E-OBS and satellite-derived, H05+P_H16 product, 1-day rainfall observations for the whole study area (red line is the 15 days moving average).

4.4 Specifications of the integrated product H05+P_H16

From the analyses performed in this study, the following specifications might be prescribed for the integrated product:

1) The use of H16 products from both Metop-A and Metop-B satellites provides a better temporal coverage and, hence, higher accuracy (results not shown of a preliminary analysis done by using only Metop-A ASCAT sensor) of the precipitation product obtained from soil moisture data (P_H16).
2) The simple nudging scheme (constant weights throughout the year) is found to perform well in accordance with previous results in Italy reported by Ciabatta et al. (2015a).
3) A time resolution of 1 day (from 00:00 to 24:00 UTC) and a spatial resolution of ~12.5 km is found to be satisfactory, even though an analysis at high spatial-temporal resolution is required but using an improved benchmark dataset with respect to E-OBS.

These specifications can be considered for a first implementation of the integrated product in the near real time chain of H-SAF project.

5 Conclusions

The current study investigated the performance of three satellite-based rainfall products, i.e., P_H16, H05, and H05+P_H16, by using E-OBS dataset as benchmark. To summarize, the products accuracy is found satisfactory, with evident benefits in using the integrated product for estimating 1-day rainfall over Europe at a spatial resolution of 12.5 km.

Notwithstanding the already good and promising results obtained in this ASA, further studies are needed for better investigating the potentials and limitations of the integrated product. Specifically, the following analyses deserve to be carried out:

1) Assessment of the spatial and temporal resolution that represent the best compromise between product accuracy and user requirements.
2) Detailed analysis of the spatial and temporal variability of parameter values included in the SM2RAIN algorithm, the exponential filter and the nudging scheme.
3) Effect of using multiple or single satellite sensors (e.g., only Metop-A or Metop-B, only microwave-based sensors) in the integration procedure.
4) Improvement of the SM2RAIN algorithm by incorporating additional components for surface runoff and evapotranspiration, by including the temporal variability of the parameter values and by considering different methods for filtering out the noise of satellite soil moisture data.
5) Improvement of the nudging scheme allowing to vary in time the parameter values and explicitly considering the error structure of the parent products (e.g., low accuracy of SM2RAIN-based product close to soil saturation conditions).

All these points will be investigated in the near future for enhancing the robustness and reliability of the integrated product that might be a new rainfall product in the next phase (CDOP-3) of H-SAF project.

Acknowledgements: We acknowledge the E-OBS dataset from the EU-FP6 project ENSEMBLES (http://ensembles-eu.metoffice.com) and the data providers in the ECA&D project (http://www.ecad.eu). We also acknowledge the support by C.N.M.C.A. and TU-Wien for the download and the use of H05 and H16 products.

6 References

Abera, W., Brocca, L., Rigon, R. (2015). Comparative evaluation of different satellite rainfall estimation products and bias correction in the Upper Blue Nile (UBN) basin. submitted to Atmospheric Research.

Albergel, C., Rüdiger, C., Carrer, D., Calvet, J.C., Fritz, N., et al. (2009). An evaluation of ASCAT surface soil moisture products with in-situ observations in southwestern France. Hydrol. Earth Syst. Sci., 13, 115-124.

ATDD-05 (2010). Algorithm Theoretical Definition Document (ATDD) for product - PR-OBS-5 - Accumulated precipitation at ground by blended MW and IR. 30 May 2010, available at: http://hsaf.meteoam.it/documents/ATDD/SAF_HSAF_ATBD-05_1_0.pdf.

ATBD-16 (2013). Algorithm Theoretical Baseline Document (ATBD) for product H16/SM-OBS-3 - Large-scale surface soil moisture by radar scatterometer. 21 October 2013, available at: http://hsaf.meteoam.it/documents/ATDD/SAF_HSAF_CDOP_ATBD-16_1_0.pdf.

Brocca, L., Hasenauer, S., Lacava, T., Melone, F., Moramarco, T., Wagner, W., Dorigo, W., Matgen, P., Martínez-Fernández, J., Llorens, P., Latron, J., Martin, C., Bittelli, M. (2011). Soil moisture estimation through ASCAT and AMSR-E sensors: an intercomparison and validation study across Europe. Remote Sens. Environ., 115(12), 3390-3408.

Brocca, L., Melone, F., Moramarco, T., Wagner, W. (2013). A new method for rainfall estimation through soil moisture observations. Geophys. Res. Lett., 40(5), 853-858.

Brocca, L., Ciabatta, L., Massari, C., Moramarco, T., Hahn, S., Hasenauer, S., Kidd, R., Dorigo, W., Wagner, W., Levizzani, V. (2014). Soil as a natural rain gauge: estimating global rainfall from satellite soil moisture data. Journal of Geophysical Research, 119(9), 5128-5141.

Brocca, L., Massari, C., Ciabatta, L., Moramarco, T., Penna, D., Zuecco, G., Pianezzola, L., Borga, M., Matgen, P., Martínez-Fernández, J. (2015a). Rainfall estimation from in situ soil moisture observations at several sites in Europe: an evaluation of SM2RAIN algorithm. Journal of Hydrology and Hydromechanics, 63(3), 201-209.

Brocca, L., Massari, C., Ciabatta, L., Wagner, W., Stoffelen, A. (2015b). Remote sensing of terrestrial rainfall from Ku-band scatterometers. submitted to IEEE Journal of Selected Topics in Applied Earth Observations and Remote Sensing.

Ciabatta, L., Brocca, L., Massari, C., Moramarco, T., Puca, S., Rinollo, A., Gabellani, S., Wagner, W. (2015a). Integration of satellite soil moisture and rainfall observations over the Italian territory. Journal of Hydrometeorology, 16(3), 1341-1355.

Ciabatta, L., Brocca, L., Massari, C., Moramarco, T., Gabellani, S., Puca, S., Wagner, W. (2015b). Rainfall-runoff modelling by using SM2RAIN-derived and state-of-the-art satellite rainfall products over Italy. International Journal of Applied Earth Observation and Geoinformation, in press, doi:10.1016/j.jag.2015.10.004

Crow, W.T., Huffman, G.F., Bindlish, R., Jackson, T.J. (2009). Improving satellite rainfall accumulation estimates using spaceborne soil moisture retrievals. J. Hydrometeorol., 10, 199-212.

Dinku, T., Ceccato, P., Grover-Kopec, E., Lemma, M., Connor, S.J., Ropelewsky, C.F. (2007). Validation of satellite rainfall products over East Africa's complex topography. Int. J. Remote Sens., 28 (7), 1503-1526.

Haylock, M.R., Hofstra, N., Klein Tank, A.M.G., Klok, E.J., Jones, P.D., New, M. (2008). A European daily high-resolution gridded dataset of surface temperature and precipitation. J. Geophys. Res., 113, D20119.

Hou, A.Y., Kakar, R.K., Neeck, S., Azarbarzin, A.A., Kummerow, C.D., Kojima, M., Oki, R., Nakamura, K., Iguchi, T. (2014). The Global Precipitation Measurement (GPM) mission. Bull. Amer. Meteor. Soc., 95, 701-722.

Kidd, C., Levizzani, V. (2011). Status of satellite precipitation retrievals. Hydrol Earth Syst Sci, 15, 1109-1116.

Kim, S., Parinussa, R. M., Liu, Y. Y., Johnson, F. M., Sharma, A. (2015). A framework for combining multiple soil moisture retrievals based on maximizing temporal correlation. Geophysical Research Letters, 42(16), 6662-6670.

Klok, E.J., Klein Tank, A.M.G. (2009). Updated and extended European dataset of daily climate observations. International Journal of Climatology, *29*(8), 1182-1191.

Kucera, P.A., Ebert, E.E., Turk, F.J., Levizzani, V., Kirschbaum, D., Tapiador, F.J., Loew, A., Borsche, M. (2013). Precipitation from space: Advancing earth system science. Bull. Amer. Meteor. Soc., 94, 365-375.

Massari, C., Brocca, L., Moramarco, T., Tramblay, Y., Didon Lescot, J.-F. (2014). Potential of soil moisture observations in flood modelling: estimating initial conditions and correcting rainfall. Advances in Water Resources, 74, 44-53.

Pellarin, T., Louvet, S., Gruhier, C., Quantin, G., Legout, C. (2013). A simple and effective method for correcting soil moisture and precipitation estimates using AMSR-E measurements. Remote Sens. Environ., 136, 28-36.

Stampoulis, D., Anagnostou, E. N. (2012). Evaluation of global satellite rainfall products over continental Europe. Journal of Hydrometeorology, 13(2), 588-603.

Tapiador, F.J., Turk, F.J., Petersen, W., Hou, A.Y., Garcia-Ortega, E., Machado, L.A.T., Angelis, C.F., Salio, P., Kidd, C., Huffman, G.J., de Castro, M. (2012). Global precipitation measurement: Methods, datasets and applications. Atmos. Res., 104-105, 70-97.

Wagner, W., Lemoine, G., Rott, H. (1999). A method for estimating soil moisture from ERS scatterometer and soil data. Remote Sens. Environ., 70, 191-207.

Wanders, N., Pan, M., Wood, E.F. (2015). Correction of real-time satellite precipitation with multi-sensor satellite observations of land surface variables. Remote Sens. Environ., 160, 206-221.